

Whole-body biodistribution and radiation dosimetry of the cannabinoid type 2 receptor ligand [11 C]-NE40 in healthy subjects

Rawaha Ahmad ¹ , Michel Koole ¹ , Nele Evens ² , Kim Serdons ² , Alfons Verbruggen ² , Guy Bormans ² , Koen Van Laere ¹

¹ Division of Nuclear Medicine, University Hospital Leuven, Leuven, Belgium

² Laboratory for Radiopharmacy, University Hospital Leuven and KU Leuven, Belgium

Corresponding author:

Rawaha Ahmad, MD

Division of Nuclear Medicine E901

University Hospital Leuven

Herestraat 49

B-3000 Leuven

Tel.: +32-16-343715

Fax: +32-16-343759

E-mail: rawaha.ahmad@uzleuven.be

Abbreviated title: Human dosimetry of [11 C]-NE40 for CB2R PET

Keywords: biodistribution, dosimetry, positron emission tomography, [11C]-NE40, CB2R

Disclosure: This manuscript is the peer-reviewed version of the article Ahmad R, Koole M, Evens N, Serdons K, Verbruggen A, Bormans G, Van Laere K. Whole-body biodistribution and radiation dosimetry of the cannabinoid type 2 receptor ligand [11C]-NE40 in healthy subjects. *Mol Imaging Biol.* 2013 Aug;15(4):384-90. doi: 10.1007/s11307-013-0626-y.

The final publication is available at

<http://link.springer.com/article/10.1007%2Fs11307-013-0626-y>



Whole-body biodistribution and radiation dosimetry of the human cannabinoid type 2 receptor ligand [11C]-NE40 in healthy subjects

Journal:	<i>Molecular Imaging & Biology</i>
Manuscript ID:	MIB-13-008-Jan-BA.R1
Manuscript Categories:	Brief Article
Date Submitted by the Author:	n/a
Complete List of Authors:	Ahmad, Rawaha; University Hospital Leuven, Division of Nuclear Medicine E901 Koole, Michel; University Hospital Leuven, Division of Nuclear Medicine E901 Evens, Nele; University Hospital Leuven, Laboratory for Radiopharmacy Serdons, Kim; University Hospital Leuven, Laboratory for Radiopharmacy Verbruggen, alfons; KULeuven, Laboratory for Radiopharmacy Bormans, Guy; K.U.Leuven, Laboratory for Radiopharmacy Van Laere, Koen; KULeuven, Nuclear Medicine
Keywords:	biodistribution, dosimetry, positron emission tomography, [11C]-NE40, CB2R

1
2
3
4
5
6
7
8
9
10
11
12
13
14
15
16
17
18
19
20
21
22
23
24
25
26
27
28
29
30
31
32
33
34
35
36
37
38
39
40
41
42
43
44
45
46
47
48
49
50
51
52
53
54
55
56
57
58
59
60

Whole-body biodistribution and radiation dosimetry of the cannabinoid type 2 receptor ligand [¹¹C]-NE40 in healthy subjects

Rawaha Ahmad ¹, Michel Koole ¹, Nele Evens ², Kim Serdons ², Alfons Verbruggen ², Guy Bormans ², Koen Van Laere ¹

¹ Division of Nuclear Medicine, University Hospital Leuven, Leuven, Belgium

² Laboratory for Radiopharmacy, University Hospital Leuven and KU Leuven, Belgium

Short title: Human dosimetry of [¹¹C]-NE40 for CB2R PET

Manuscript category: Brief article

To be submitted to: Molecular imaging and Biology

* Corresponding author:

Rawaha Ahmad, MD

Division of Nuclear Medicine E901

University Hospital Leuven

Herestraat 49

B-3000 Leuven

Tel.: +32-16-343715

Fax: +32-16-343759

E-mail: rawaha.ahmad@uzleuven.be

Abstract

Purpose: The type 2 cannabinoid receptor (CB2R) is part of the human endocannabinoid system and is involved in central and peripheral inflammatory processes. *In vivo* imaging of the CB2R would allow study of several (neuro)inflammatory disorders. In this study we have investigated the safety and tolerability of [¹¹C]-NE40, a CB2R PET ligand, in healthy human male subjects, and determined its biodistribution and radiation dosimetry.

Procedure: Six healthy male subjects (age 20-65 years) underwent a dynamic series of 9 whole-body PET/CT scans for up to 140 minutes, after injection of an average bolus 286 MBq of [¹¹C]-NE40. Organ absorbed and total effective doses were calculated through OLINDA.

Results: [¹¹C]-NE40 showed high initial uptake in the spleen and a predominant hepatobiliary excretion. In the brain, rapid uptake and swift washout was seen. Organ absorbed doses were largest for small intestine and liver, with 15.6 and 11.5 μGy/MBq, respectively. The mean effective dose was 3.64 ± 0.81 μSv/MBq. There were no changes with ageing observed. No adverse events were encountered.

Conclusions: This first-in-man study of [¹¹C]-NE40 showed an expected biodistribution compatible with lymphoid tissue uptake and appropriate fast brain kinetics in the healthy human brain, underscoring the potential of this tracer for further application in central and peripheral inflammation imaging. The ED is within the typical expected range for ¹¹C ligands.

Key words: biodistribution, dosimetry, positron emission tomography, [¹¹C]-NE40, CB2R

Introduction

The type 2 cannabinoid receptor (CB2R), isolated and structurally characterized in the early nineties of the past century [1], is part of the endocannabinoid system (ECS), together with the type 1 (CB1R) receptor. Both the [cannabinoid type 1 \(CB1R\)](#) and CB2R are G-protein coupled receptors (GPCR's), that are quite divergent in structure with only 44% overall homology [2]. In contrast to the CB1R, which is the most abundant GPCR in the central nervous system (CNS), the CB2R is widely expressed in immune-related tissues and organs, with high expression levels in spleen, tonsils and leucocytes [3]. Outside the immune system, CB2R is expressed to a lesser extent in salivary gland, skeletal muscle, pancreas, ovary and testis [4-8]. In non-pathological conditions, cerebral CB2R expression is very low and only present in the cerebellum and pons [9-10]. CB2Rs are upregulated in inflammatory conditions by activated microglia, are involved in the production of nitric oxide (NO) and cytokines [11]. Furthermore, the CB2R is involved in pain processing [12].

There is accumulating evidence that the ECS is involved in the pathogenesis and clinical expression of neurodegenerative disorders, in part through the process of neuroinflammation [13-14]. Upregulation of CB2R has been described postmortem in patients with Alzheimer's disease (AD) [15], Huntington's disease (HD) [16] and Parkinson's disease (PD) [17]. Therefore, positron emission tomography (PET) imaging of CB2R in the CNS can provide a tool to investigate the in vivo importance of CB2R in central inflammatory disorders.

Whereas several PET radioligands have been validated for the CB1R [18-20], only more recently attempts to radiolabel probes for CB2R have been undertaken [21]. A carbon-11-labeled CB2-selective PET tracer was described but without penetration of the blood-brain-barrier (BBB) [22-23], limiting its applicability to peripheral visualization of the CB2R. Recently, we have developed and validated novel specific radioligand for CB2R PET, 2-oxo-

1
2
3
4
5
6
7 7-[¹¹C]-methoxy-8butyloxy-1,2-dihydroquinoline-3-carboxylic acid cyclohexylamide ([¹¹C]-
8 NE40). This PET ligand is fairly lipophilic (distribution coefficient (logD) of 3.9 and total
9 polar surface area (tPSA) of 80.42 Å²) [24]. In vitro ligand binding studies using Chinese
10 hamster ovary (CHO)-cells expressing the human CB2R have shown that NE40 has a
11 relatively high binding affinity (K_i = 9.6 nM), which was confirmed by in vivo CB2R binding
12 in mouse spleen [22, 24], and high specificity (100-fold over the CB1R). Radioligand safety
13 was investigated by toxicity studies including genotoxicity (Ames test) and histopathologic
14 evaluation in rats [25] under the microdosing concept [26]. In vivo binding in a rat model with
15 adeno-associated viral human CB2R overexpression was confirmed [27]. Here we describe
16 the first-in-man imaging studies, with safety and dosimetry assessment in both young and
17 elderly male volunteers.
18
19
20
21
22
23
24
25
26
27
28
29
30

31 **Materials and methods**

32 Subjects

33
34
35
36 Healthy subjects were recruited in response to an advertisement in a local community
37 newspaper. Six healthy Caucasian male subjects were included in the study. Table 1 shows
38 the demographic data. The subjects did not have any clinical significant medical or
39 neurological history, and they did not have any clinically significant abnormality on physical,
40 neurological, or laboratory examinations. In addition, they were not taking any anti-
41 inflammatory medication at the moment of the scan or during at least four weeks before the
42 scan. The study was approved by the local Ethics Committee and conducted according to the
43 latest guidelines of the Declaration of Helsinki. Written informed consent was obtained from
44 all volunteers before the start of their study.
45
46
47
48
49
50
51
52

53 Radiotracer characteristics and preparation [¹¹C]-NE40

1
2
3
4
5
6
7 Radiotracer preparation was performed as described previously [24]. In short, a stream of
8 helium containing [^{11}C]- CH_3I was bubbled through a solution of 200 μg 2-oxo-7-hydroxy-8-
9 butyloxy-1,2-dihydroquinoline-3-carboxylic acid cyclohexylamide and 2–4 miligram Cs_2CO_3
10 in 200 μl dimethylformamide. The reaction mixture was heated and diluted. The radiolabeled
11 compound [^{11}C]-NE40 was collected using reversed-phase high performance liquid
12 chromatography (HPLC). After formulation, the identity, chemical and radiochemical purity
13 of the tracer agent [^{11}C]-NE40 were checked using HPLC. Specific activity was 363 (range
14 200-632) $\text{GBq}/\mu\text{mol}$; the maximum amount of cold NE40 injected was < 1.0 (range 0.4-0.9)
15 μg .
16
17
18
19
20
21
22
23

24 25 26 PET/CT procedure

27
28 All subjects fasted for at least 6 hours before PET. Subjects underwent a dynamic series of 9
29 whole-body PET-CT scans on a Hirez Biograph 16 PET/CT (Siemens, Erlangen, Germany)
30 after bolus I.V. injection of 286 MBq (range 201-325 MBq) of [^{11}C]-NE40. Data were
31 acquired with a single energy window set at 425 to 650 keV. The first PET segment
32 (sequential acquisition of WB scan 1 to 8) started simultaneously with the bolus injection and
33 lasted for 60 minutes (time per bed position 30 s (for WB1-3), 60 s (for WB4-6) and 120 s
34 (for WB7-8)). The second segment (WB9) started at 120 minutes post-injection at 4 minutes
35 per bed position. A low-dose CT (tube potential 80 kV; 11 mAs) was performed before each
36 scan segment (The additional effective dose from this CT is 0.5 mSv (CT-Expo version 1.7,
37 male phantom), so the subject underwent an estimated additional radiation burden of 1.0 mSv
38 on top of the PET study). At our center, daily quality control (QC) of the PET system is
39 performed using a uniform ^{68}Ge cylinder to check the uniformity and the stability of the
40 system. Cross calibration with the dose calibrator is performed at least every 3 months using
41 a uniform ^{18}F cylinder [28]. Moreover, we work according to the EARL FDG PET/CT
42
43
44
45
46
47
48
49
50
51
52
53
54
55
56
57
58
59
60

Formatted: Font: (Default) Times New Roman, 12 pt

Formatted: Font: Times New Roman, 12 pt

Formatted: Font: Times New Roman, 12 pt

1
2
3
4
5
6 accreditation program (ResEARCh for Life).

7 http://earl.eanm.org/cms/website.php?id=en/projects/fdg_pet_ct_accreditation.htm.

8
9
10
11
12
13
14
15
16
17
18
19
20
21
22
23
24
25
26
27
28
29
30
31
32
33
34
35
36
37
38
39
40
41
42
43
44
45
46
47
48
49
50
51
52
53
54
55
56
57
58
59
60

Formatted: Font: (Default) Times New Roman, 12 pt

Formatted: Font: Times New Roman, 12 pt

Formatted: Font: Times New Roman, 12 pt

Whole-body images were reconstructed using a three-dimensional (3D) ordered-subset expectation maximization (OSEM) iterative reconstruction, with 5 iterations and 8 subsets, with CT-based attenuation and scatter correction by standard vendor-based reconstruction. No partial volume effect correction was performed.

Urine was collected after each scan segment for total urinary bladder activity determination and up to 3 hours post injection. Volume was determined by weighing the amount of urine and activity concentration was determined by measuring the activity of a defined volumetric sample of 1 ml with a well counter Wallac 1480 wizard 14 inch (Perkin Elmer, Turku, Finland).

Safety was assessed through physical and neurological examination, vital parameter assessment, electrocardiogram (ECG), laboratory testing, and monitoring of subjective adverse experiences with telephone follow-up 24 hours and 14 days post-injection.

Data Analysis

Data were analyzed and reported according to the EANM guidelines for clinical dosimetry reporting [29]. Reconstructed data were analyzed using PMOD software (version 3.0; PMOD Inc., Zurich). Three dimensional VOIs were constructed on the PET emission images to include all organ activity, and their position was verified on corresponding CT images, as described previously [30]. The following organs with significant visualized activity were included as source organs: brain, gallbladder, intestines, heart, kidneys, liver, lungs, red marrow, spleen, thyroid and urinary bladder. Total tracer retention as a function of time or time-activity curves (TACs) was determined. To account for the differences in timing of each bed position, the corresponding acquisition times were calculated for each source organ, taking the bed position of the axial midposition of the organ under consideration on the

1
2
3
4
5
6
7 corresponding CT scout image on which bed positions with spatial overlap are indicated.

8 Specifically, for the axial red marrow, the midlumbar vertebral position was taken as the
9 average time value. In this way, time-activity curves were calculated for each of the source
10 organs indicated earlier.
11
12
13

14
15 To determine preliminary kinetics of brain and spleen uptake, mean standard uptake value
16 (SUV) TACs for brain and spleen were generated.
17
18

19 Organ time-integrated activity coefficients (previously named 'residence times' [31]) were
20 computed by calculating the area under the time-activity curve (TAC) of each source organ
21 through curve fitting. Different models for different organs were used, depending on their
22 kinetics (standardly, a bi-exponential curve was taken when the first data point was already
23 the maximum activity point; in other cases an extra factor or term $(1 - \exp(-\ln(2) \times T/T_i))$ was
24 included to produce a better fit with a specific maximum). For heart wall, kidneys, spleen and
25 thyroid a bi-exponential was fitted, while a mono-exponential could be used for the lungs. To
26 account for the tracer uptake phase in brain and liver, the function $A_1 \times (1 - \exp(-\ln(2) \times T/T_1)) \times$
27 $\exp(-\ln(2) \times T/T_2)$ was fitted to the TAC while the function $A_1 \times (1 - \exp(-\ln(2) \times T/T_1)) \times \exp(-$
28 $\ln(2) \times T/T_2) + A_2 \times \exp(-\ln(2) \times T/T_{e3})$ was used to model the TAC of gallbladder, red marrow
29 and remainder.
30
31
32
33
34
35
36
37
38
39
40

41 The ICRP 30 gastrointestinal (GI) model [32] was used to determine the time-integrated
42 activity coefficients for the organs involved in the gastrointestinal tract while the voiding
43 bladder model with a voiding interval of 2 hours was used to estimate the time-integrated
44 activity coefficient for the urinary bladder (UB) [33]. The fraction of injected activity entering
45 the small intestines was estimated by fitting the exponential $A_{GI1} + A_{GI2} \times (1 - \exp(-\ln(2) \times T/T_{GI}))$
46 to the decay corrected TAC of the intestinal VOI. Total fraction for the gastrointestinal tract
47 was determined as $(A_{GI1} + A_{GI2})$ normalized to injected activity A_{inj} . The remaining fraction of
48
49
50
51
52
53
54
55
56
57
58
59
60

1
2
3
4
5
6
7 the injected activity was considered as excreted through the urinary bladder. Biological half-
8 life for the fraction entering the urinary bladder was estimated by fitting $(A_{inj}-A_{GI1}-A_{GI2}) \times (1-$
9 $\exp(-\ln(2) \times T/T_{UB}))$ to the TAC of the urinary bladder corrected for decay and between scan
10 voiding. Radiation exposure of the body and critical organs were calculated from the tracer
11 time-integrated activity coefficients using the OLINDA (Organ Level Internal Dose
12 Assessment, Vanderbilt University, USA) software package. The effective dose (ED) was
13 calculated from the individual organ doses with a predefined weighting factor for each of the
14 source organs [34].
15
16
17
18
19
20
21
22

23 Results

24
25 As for safety, all monitored clinical parameters (heart rate, blood pressure, 12-lead
26 electrocardiogram, blood analysis) remained normal and no clinically significant adverse
27 experiences were reported by the subjects at the time of scanning, nor were any reported
28 during the follow-up phone interviews.
29
30
31
32

33
34 Figure 1 shows a series of coronal and sagittal whole-body slices of [^{11}C]-NE40 over time for
35 a representative subject. The tracer was readily taken up in the liver and partially excreted
36 through the gastrointestinal system. Some urinary tract activity was noted after a few minutes.
37
38 Based on the statistics of the abdominal VOI, $10.5 \pm 7.5\%$ of the injected activity was entering
39 the intestines and therefore considered as cleared hepatobiliary. The remaining fraction was
40 considered excreted through the urinary tract, with a biological urinary clearance half-life
41 estimated at 183 ± 96 hours. Due to the slow urinary excretion rate, collected urinal activity
42 from the first two patients during 3 hours post injection was very limited and therefore was
43 not further taken into account for the calculations. Rapid uptake (to a maximum of 1.5- 3% of
44 the injected activity) and fast washout in the brain was seen, in accordance with the low
45 CB2R expression levels in normal brain.
46
47
48
49
50
51
52
53
54
55
56
57
58
59
60

1
2
3
4
5
6
7
8
9
10
11
12
13
14
15
16
17
18
19
20
21
22
23
24
25
26
27
28
29
30
31
32
33
34
35
36
37
38
39
40
41
42
43
44
45
46
47
48
49
50
51
52
53
54
55
56
57
58
59
60

Figure 2 shows relative time-activity curves for the liver, brain, gallbladder and spleen after injection of [¹¹C]-NE40. The highest variability in activity was observed in the gallbladder.

In one of the subjects we observed a second peak of activity after 40 minutes post-injection (p.i.).

Time-integrated activity coefficients for all individual patients and source organs are given in Supplementary Table 1. Table 2 summarizes organ mean radiation absorbed doses and the effective doses. Individual organ absorbed ~~doses~~doses; average organ doses derived from individual doses as well as based on mean kinetic parameters (time-integrated activity coefficient TIAC) and their relative difference (%) are given in Supplemental Table 2. As can be seen from this table, there is only a very small difference between both approaches. The small intestine and the liver showed the highest organ dose of 15.6 and 11.5 μGy/MBq, respectively, followed by the heart wall (7.02 μGy/MBq). Table 1 includes the individual ED estimates for all subjects. The average ED was 3.64 ± 0.81 μSv/MBq (range 2.79 to 5.09 μSv/MBq). No significant correlation between age and ED was found.

Figure 3 shows the time activity curves (standard uptake values, SUV) with activity values corrected for decay caused by the time interval between tracer injection and start time of the different whole body PET scans of the six healthy volunteers for the brain and the spleen. In the brain, a maximum between 10-20 min can be seen in some subjects, with thereafter a continuous decline of the SUV value. In the spleen, after 20 minutes a stable SUV is seen, plateauing around 1.

Discussion

Biomarkers of (neuro)inflammation can be useful as a tool in drug development and in clinical conditions for severity assessment and therapy follow-up. The CB2R is predominantly expressed in peripheral tissues and shows the highest expression levels in

1
2
3
4
5
6
7 organs of the immune system [35]. In the central nervous system, CB2R is upregulated in
8
9 inflammatory conditions of activated microglia. Most of the CB2R radioligands described so
10
11 far are derivatives of 2-oxoquinoline class that have shown a high selectivity for CB2Rs as
12
13 inverse agonists [22-24, 36-37]. Although some were promising in *in vitro* studies, their
14
15 *in vivo* stability was poor with fast metabolism. Proof-of-principle of the feasibility of CB2R
16
17 imaging in pathological conditions with a neuroinflammatory component *in vivo* was
18
19 described by Horti et al. [21]. Since [¹¹C]-NE40 showed favourable characteristics for
20
21 neuroimaging, we performed this first-in-man study to assess the biodistribution and evaluate
22
23 the safety of [¹¹C]-NE40.

24
25 The gallbladder showed the highest variability in activity. In one of the subjects we observed
26
27 a second peak of activity after 40 minutes p.i., possibly due to an early contraction of the
28
29 gallbladder, after which there is an accumulation of the activity with a second contraction.
30
31 Overall the gallbladder activity can differ between subjects due to large differences in the
32
33 individual kinetics of gallbladder emptying, a process influenced by multiple hormonal
34
35 factors and gastrointestinal interactions.

36
37 The average injected tracer mass dose in this study was less than 1.0 µgram. There were no
38
39 subjective effects or adverse events including changes in laboratory blood tests, blood
40
41 pressure, pulse and ECG. The subjects in this study received a total ED of 2.1 mSv including
42
43 the PET and attenuation correction CT studies. In a recent literature overview of 32 human
44
45 PET radiation dosimetry studies with ¹¹C radioligands, van der Aart et al. showed that the vast
46
47 majority have an effective dose of below 9 µSv/MBq, with a mean of 5.9 µSv/MBq [38]. The
48
49 effective radiation dose in our study is thus less than this average, moreover indicating that
50
51 multiple PET scans can be performed in the same subject within conventionally accepted
52
53 dose limits (class IIA WHO of 10 mSv), allowing its use in drug development and follow-up
54
55 studies.

Conclusion

[¹¹C]-NE40 results in an effective human radiation dose of 3.64 μSv/MBq, which is in the lower end of the range of ¹¹C- tracers. The biodistribution with spleen uptake and absence of fixed brain uptake in healthy conditions makes the tracer promising for further studies in pathological conditions.

References

1. Munro S, Thomas KL, Abu-Shaar M (1993) Molecular characterization of a peripheral receptor for cannabinoids. *Nature* 365:61-65.
2. Felder CC, Joyce KE, Briley EM, et al. (1995) Comparison of the pharmacology and signal transduction of the human cannabinoid CB1 and CB2 receptors. *MolPharmacol* 48:443-450.
3. Lynn AB, Herkenham M (1994) Localization of cannabinoid receptors and nonsaturable high-density cannabinoid binding sites in peripheral tissues of the rat: implications for receptor-mediated immune modulation by cannabinoids. *J PharmacolExpTher* 268:1612-1623.
4. Prestifilippo JP, Fernandez-Solari J, de la Cal C, et al. (2006) Inhibition of salivary secretion by activation of cannabinoid receptors. *ExpBiolMed(Maywood)* 231:1421-1429.
5. Cavuoto P, McAinch AJ, Hatzinikolas G, Janovska A, Game P, Wittert GA (2007) The expression of receptors for endocannabinoids in human and rodent skeletal muscle. *BiochemBiophysResCommun* 364:105-110.
6. Bermudez-Silva FJ, Suarez J, Baixeras E, et al. (2008) Presence of functional cannabinoid receptors in human endocrine pancreas. *Diabetologia* 51:476-487.

Formatted: Font: Not Italic

Formatted: Line spacing: Double, Border: Bottom: (No border)

- 1
2
3
4
5
6
7
8
9
10
11
12
13
14
15
16
17
18
19
20
21
22
23
24
25
26
27
28
29
30
31
32
33
34
35
36
37
38
39
40
41
42
43
44
45
46
47
48
49
50
51
52
53
54
55
56
57
58
59
60
7. El-Talatini MR, Taylor AH, Elson JC, Brown L, Davidson AC, Konje JC (2009) Localisation and function of the endocannabinoid system in the human ovary. *PLoS ONE* 4:e4579.
8. Liu QR, Pan CH, Hishimoto A, et al. (2009) Species differences in cannabinoid receptor 2 (CNR2 gene): identification of novel human and rodent CB2 isoforms, differential tissue expression and regulation by cannabinoid receptor ligands. *Genes Brain Behav* 8:519-530.
9. Onaivi ES (2006) Neuropsychobiological evidence for the functional presence and expression of cannabinoid CB2 receptors in the brain. *Neuropsychobiology* 54:231-246.
10. Van Sickle MD, Duncan M, Kingsley PJ, et al. (2005) Identification and functional characterization of brainstem cannabinoid CB2 receptors. *Science* 310:329-332.
11. Ehrhart J, Obregon D, Mori T, et al. (2005) Stimulation of cannabinoid receptor 2 (CB2) suppresses microglial activation. *JNeuroinflammation* 2:29.
12. Curto-Reyes V, Llamas S, Hidalgo A, Menendez L, Baamonde A Spinal and peripheral analgesic effects of the CB2 cannabinoid receptor agonist AM1241 in two models of bone cancer-induced pain. *BrJPharmacol* 160:561-573.
13. Bisogno T, Di Marzo V (2008) The role of the endocannabinoid system in Alzheimer's disease: facts and hypotheses. *Curr Pharm Des* 14:2299-3305.
14. Pazos MR, Sagredo O, Fernandez-Ruiz J (2008) The endocannabinoid system in Huntington's disease. *Curr Pharm Des* 14:2317-2325.
15. Benito C, Nunez E, Tolon RM, et al. (2003) Cannabinoid CB2 receptors and fatty acid amide hydrolase are selectively overexpressed in neuritic plaque-associated glia in Alzheimer's disease brains. *J Neurosci* 23:11136-11141.
16. Palazuelos J, Aguado T, Pazos MR, et al. (2009) Microglial CB2 cannabinoid receptors are neuroprotective in Huntington's disease excitotoxicity. *Brain* 132:3152-3164.

1
2
3
4
5
6
7
8
9
10
11
12
13
14
15
16
17
18
19
20
21
22
23
24
25
26
27
28
29
30
31
32
33
34
35
36
37
38
39
40
41
42
43
44
45
46
47
48
49
50
51
52
53
54
55
56
57
58
59
60

17. Price DA, Martinez AA, Seillier A, et al. (2009) WIN55,212-2, a cannabinoid receptor agonist, protects against nigrostriatal cell loss in the 1-methyl-4-phenyl-1,2,3,6-tetrahydropyridine mouse model of Parkinson's disease. *Eur J Neurosci* 29:2177-2186.
18. Burns HD, Van Laere K, Sanabria-Bohorquez S, et al. (2007) [18F]MK-9470, a positron emission tomography (PET) tracer for in vivo human PET brain imaging of the cannabinoid-1 receptor. *Proc Natl Acad Sci USA* 104:9800-9805.
19. Donohue SR, Varnas K, Jia Z, Gulyas B, Pike VW, Halldin C (2009) Synthesis and in vitro autoradiographic evaluation of a novel high-affinity radioiodinated ligand for imaging brain cannabinoid subtype-1 receptors. *Bioorg Med Chem Lett* 19:6209-6212.
20. Horti AG, Van Laere K (2008) Development of radioligands for in vivo imaging of type 1 cannabinoid receptors (CB1) in human brain. *Curr Pharm Des* 14:3363-3383.
21. Horti AG, Gao Y, Ravert HT, et al. (2010) Synthesis and biodistribution of [11C]A-836339, a new potential radioligand for PET imaging of cannabinoid type 2 receptors (CB2). *Bioorganic & medicinal chemistry* 18:5202-5207.
22. Evens N, Bosier B, Lavey BJ, et al. (2008) Labelling and biological evaluation of [(11C)methoxy-Sch225336: a radioligand for the cannabinoid-type 2 receptor. *Nucl Med Biol* 35:793-800.
23. Gao M, Wang M, Miller KD, Hutchins GD, Zheng QH (2010) Synthesis and in vitro biological evaluation of carbon-11-labeled quinoline derivatives as new candidate PET radioligands for cannabinoid CB2 receptor imaging. *Bioorganic & medicinal chemistry* 18:2099-2106.
24. Evens N, Muccioli GG, Houbrechts N, et al. (2009) Synthesis and biological evaluation of carbon-11- and fluorine-18-labeled 2-oxoquinoline derivatives for type 2 cannabinoid receptor positron emission tomography imaging. *Nucl Med Biol* 36:455-465.

25. Evens N, Vandeputte C, Coolen C, et al. (2012) Preclinical evaluation of [11C]NE40, a type 2 cannabinoid receptor PET tracer. *NuclMedBiol* 39:389-399.
26. Ames BN, McCann J, Yamasaki E (1975) Methods for detecting carcinogens and mutagens with the Salmonella/mammalian-microsome mutagenicity test. *MutatRes* 31:347-364.
27. Evens N, Vandeputte C, Muccioli GG, et al. (2011) Synthesis, in vitro and in vivo evaluation of fluorine-18 labelled FE-GW405833 as a PET tracer for type 2 cannabinoid receptor imaging. *Bioorganic & medicinal chemistry* 19:4499-4505.
28. Boellaard R, O'Doherty MJ, Weber WA, et al. (2010) FDG PET and PET/CT: EANM procedure guidelines for tumour PET imaging: version 1.0. *European journal of nuclear medicine and molecular imaging* 37:181-200.
29. Lassmann M, Chiesa C, Flux G, Bardies M, Committee ED (2011) EANM Dosimetry Committee guidance document: good practice of clinical dosimetry reporting. *European journal of nuclear medicine and molecular imaging* 38:192-200.
30. Van Laere K, Koole M, Sanabria Bohorquez SM, et al. (2008) Whole-body biodistribution and radiation dosimetry of the human cannabinoid type-1 receptor ligand 18F-MK-9470 in healthy subjects. *JNuclMed* 49:439-445.
31. Bolch WE, Eckerman KF, Sgouros G, Thomas SR (2009) MIRD pamphlet No. 21: a generalized schema for radiopharmaceutical dosimetry--standardization of nomenclature. *J Nucl Med* 50:477-484.
32. Protection ICoR (1979) *Limits for Intakes of Workers* New York: Pergamon Press.
33. Cloutier RJ, Smith SA, Watson EE, Snyder WS, Warner GG (1973) Dose to the fetus from radionuclides in the bladder. *Health physics* 25:147-161.
34. Icrp (1991) *ICRP Publication 60 : Recommendations of the International Commission on Radiological Protection*. Oxford, UK: Pergamon Press.

1
2
3
4
5
6
7
8
9
10
11
12
13
14
15
16
17
18
19
20
21
22
23
24
25
26
27
28
29
30
31
32
33
34
35
36
37
38
39
40
41
42
43
44
45
46
47
48
49
50
51
52
53
54
55
56
57
58
59
60

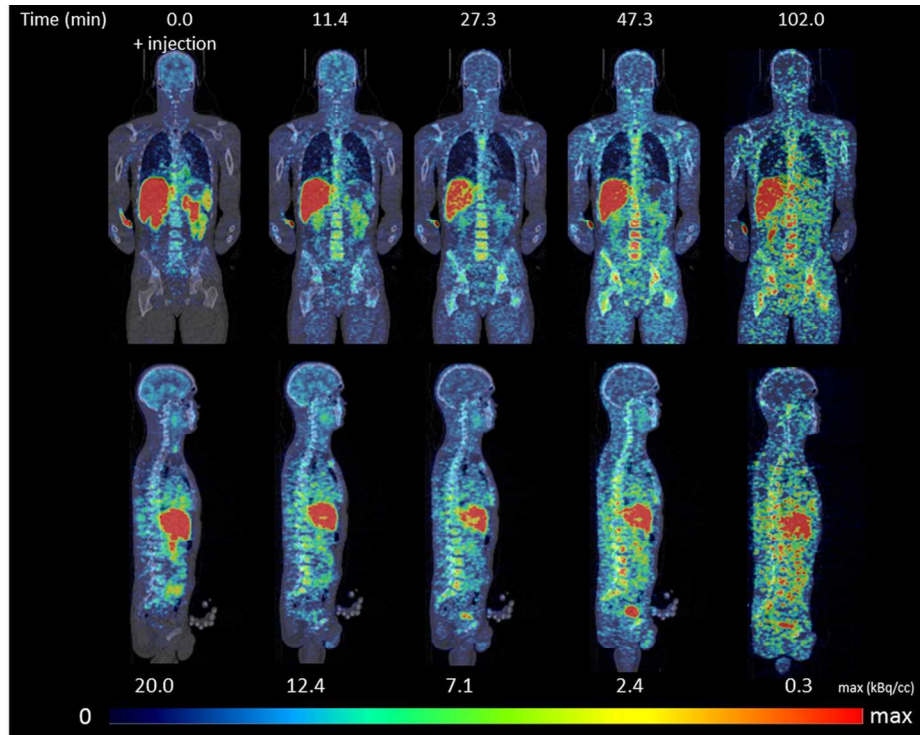
35. Maccarrone M, Battista N, Centonze D (2007) The endocannabinoid pathway in Huntington's disease: A comparison with other neurodegenerative diseases. *ProgNeurobiol* 81:349-379.
36. Raitio KH, Savinainen JR, Nevalainen T, Jarvinen T, Vepsalainen J (2006) Synthesis and in vitro evaluation of novel 2-oxo-1,2-dihydroquinoline CB2 receptor inverse agonists. *ChemBiolDrug Des* 68:334-340.
37. Turkman N, Shavrin A, Paolillo V, et al. Synthesis and preliminary evaluation of [18F]-labeled 2-oxoquinoline derivatives for PET imaging of cannabinoid CB2 receptor. *NuclMedBiol* 39:593-600.
38. van der Aart J, Hallett WA, Rabiner EA, Passchier J, Comley RA Radiation dose estimates for carbon-11-labelled PET tracers. *NuclMedBiol* 39:305-314.

Figure Legends

Figure 1: Whole-body coronal and mid-sagittal PET-CT sections of [^{11}C]-NE40 in subject 2 (uncorrected for decay, in kBq/cc). Data are normalized in the same scale on a maximum activity given in the bottom row, in order to better visualize the relative distribution. Upper row indicates start time (min) of whole-body scan.

Figure 2: Mean activity over time in brain, spleen, liver and gallbladder as fraction of total-body activity for all subjects.

Figure 3: ~~Decay corrected~~ Time activity curves (expressed in standard uptake value (SUV); activity values decay corrected relative to the time of tracer injection) of the spleen and the brain for the 6 volunteers.



32
33
34
35
36
37
38
39
40
41
42
43
44
45
46
47
48
49
50
51
52
53
54
55
56
57
58
59
60

Figure 1: Whole-body coronal and mid-sagittal PET-CT sections of [11C]-NE40 in subject 2 (uncorrected for decay, in kBq/cc). Data are normalized in the same scale on a maximum activity given in the bottom row, in order to better visualize the relative distribution. Upper row indicates start time (min) of whole-body scan.
114x85mm (300 x 300 DPI)

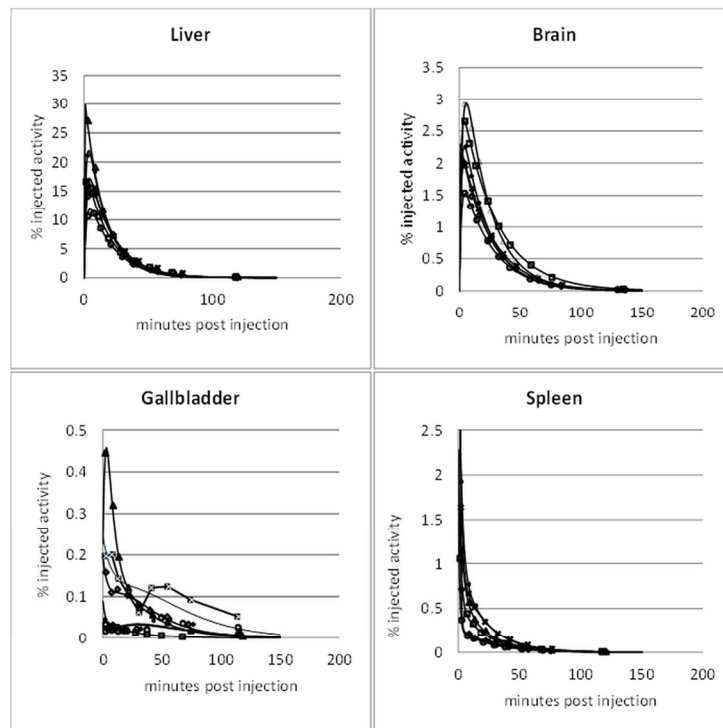


Figure 2: Mean activity over time in brain, spleen, liver and gallbladder as fraction of total-body activity for all subjects.

114x85mm (300 x 300 DPI)

1
2
3
4
5
6
7
8
9
10
11
12
13
14
15
16
17
18
19
20
21
22
23
24
25
26
27
28
29
30
31
32
33
34
35
36
37
38
39
40
41
42
43
44
45
46
47
48
49
50
51
52
53
54
55
56
57
58
59
60

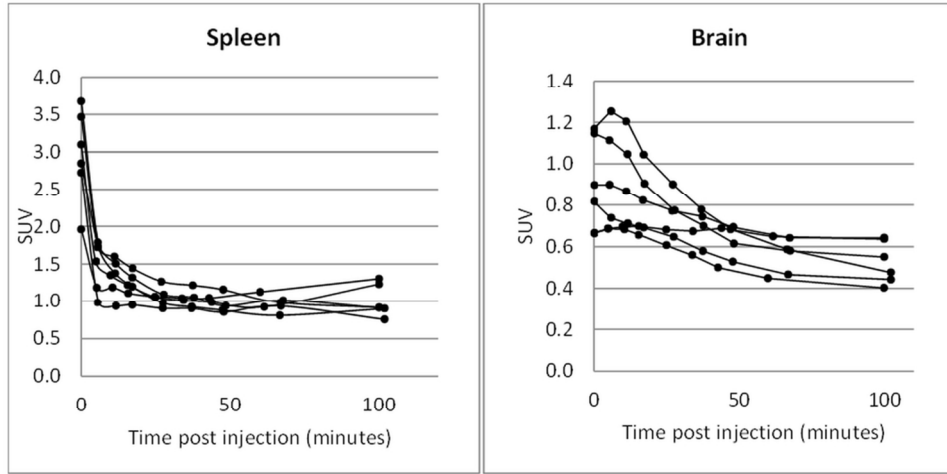


Figure 3: Time activity curves (expressed in standard uptake value (SUV); activity values decay corrected relative to the time of tracer injection) of the spleen and the brain for the 6 volunteers.
114x85mm (300 x 300 DPI)

view

Table 1. Subject Data, net injected activity of [¹¹C]-NE40, and individual effective dose

Subject	Sex	Age (y)	Height (cm)	Mass (kg)	Body mass index (kg/m ²)	Injected activity (MBq)	Individual ED (μSv/MBq)
HV_1	M	20.8	178	61	19.3	302.3	3.93
HV_2	M	44.9	187	90	25.7	201.2	2.79
HV_3	M	24.2	186	86	24.8	254.8	3.05
HV_4	M	65.3	166	61	22.1	310.1	5.09
HV_5	M	61.0	187	90	25.7	324.1	3.46
HV_6	M	22.6	192	82	22.2	325.8	3.54
Mean ± SD		39.8±20.1	182.7±9.3	78.3±13.8	23.3±2.6	286±49	3.64±0.81

HV: healthy volunteer, M: male, y: year, SD: standard deviation, ED: effective dose

Table 2: Radiation absorbed dose estimate (OLINDA) Based on ICRP 30 gastrointestinal tract model

Target Organ	Mean Absorbed Dose ($\mu\text{Gy}/\text{MBq}$)	Coefficient of variation (%)
Adrenals	2.71 ± 0.394	14.1
Brain	2.73 ± 0.84	30.7
Breasts	1.547 ± 0.293	20.1
Gallbladder Wall	5.82 ± 0.13	21.8
Lower Large Intestine Wall	2.62 ± 0.10	38.8
Small Intestine	15.6 ± 1.03	65.7
Stomach Wall	2.263 ± 0.514	22.8
Upper large intestine Wall	6.657 ± 3.83	57.6
Heart Wall	7.02 ± 2.273	32.4
Kidneys	6.657 ± 1.53	23.0
Liver	11.5 ± 1.152	10.0
Lungs	4.01 ± 0.697	17.2
Muscle	1.758 ± 0.41	23.4
Pancreas	2.72 ± 0.43	15.8
Red Marrow	5.071 ± 0.93	18.4
Osteogenic Cells	4.283 ± 1.00	23.4
Skin	1.31 ± 0.31	23.5
Spleen	6.01 ± 1.31	21.8
Testes	1.42 ± 0.364	25.2
Thymus	1.768 ± 0.34	19.3
Thyroid	4.283 ± 1.32	30.9
Urinary Bladder Wall	2.44 ± 0.768	31.2
Uterus	2.768 ± 1.10	39.7
Total Body	2.40 ± 0.51	21.3
Effective dose ($\mu\text{Sv}/\text{MBq}$)	$3.64E \pm 0.81$	22.3

Data are mean \pm SD

1
2
3
4
5
6
7
8
9
10
11
12
13
14
15
16
17
18
19
20
21
22
23
24
25
26
27
28
29
30
31
32
33
34
35
36
37
38
39
40
41
42
43
44
45
46
47
48
49
50
51
52
53
54
55
56
57
58
59
60

(SUPPLEMENTAL TABLES)

**Whole-body biodistribution and radiation dosimetry of the cannabinoid type 2 receptor
ligand [¹¹C]-NE40 in healthy subjects**

Rawaha Ahmad, Michel Koole, Nele Evens, Kim Serdons, Alfons Verbruggen, Guy
Bormans, Koen Van Laere

Formatted: Dutch (Belgium)

To be submitted to: Molecular imaging and Biology

*** Corresponding author:**

Rawaha Ahmad, MD

Division of Nuclear Medicine E901

University Hospital Leuven

Herestraat 49

B-3000 Leuven

Tel.: +32-16-343715

Fax: +32-16-343759

E-mail: rawaha.ahmad@uzleuven.be

1
2
3
4
5
6
7
8
9
10
11
12
13
14
15
16
17
18
19
20
21
22
23
24
25
26
27
28
29
30
31
32
33
34
35
36
37
38
39
40
41
42
43
44
45
46
47
48
49
50
51
52
53
54
55
56
57
58
59
60

Supplemental Table 1: Time-integrated activity coefficients (‘residence times’ – in hours)
for the individual subjects, as obtained by multiexponential curve fitting

Subject Nr.	1	2	3	4	5	6	mean	SD
Brain	0.0145	0.0095	0.0136	0.0077	0.0098	0.0098	0.0108	0.002638
Gallbladder	0.0002	0.0011	0.0015	0.0006	0.0006	0.0019	0.0010	0.000647
Lower Large Intestine	0.0001	0.0001	0.0001	0.0005	0.0002	0.0002	0.0002	0.000155
Small Intestines	0.0320	0.0217	0.0301	0.1116	0.0413	0.0385	0.0459	0.032927
Upper Large Intestine	0.0038	0.0026	0.0036	0.0132	0.0049	0.0045	0.0054	0.003887
Heart Wall	0.0042	0.0139	0.0074	0.0077	0.0060	0.0052	0.0074	0.003422
Kidneys	0.0046	0.0046	0.0065	0.0048	0.0057	0.0096	0.0060	0.001956
Liver	0.0613	0.0660	0.0819	0.0499	0.0729	0.0699	0.0670	0.010863
Lungs	0.0099	0.0099	0.0113	0.0128	0.0140	0.0136	0.0119	0.001817
Red Marrow	0.0275	0.0373	0.0310	0.0335	0.0380	0.0361	0.0339	0.004057
Spleen	0.0026	0.0051	0.0032	0.0014	0.0048	0.0046	0.0036	0.001467
Thyroid	0.0002	0.0002	0.0003	0.0003	0.0006	0.0003	0.0003	0.000151
Urinary Bladder	0.0011	0.0006	0.0013	0.0015	0.0004	0.0007	0.0009	0.000432
Remainder	0.2569	0.2217	0.2014	0.2304	0.2033	0.2146	0.2214	0.020578

Supplemental table 2: Individual organ doses (OLINDA) (mGy/MBq) for the 6 subjects (as defined in Table 1) of the study, and average organ doses derived from individual doses as well as based on mean kinetic parameters (time-integrated activity coefficients (TIAC)) and their relative difference (%).

Formatted: Line spacing: Double

Subject Nr.	1	2	3	4	5	6
Adrenals	3.21E-03	2.38E-03	2.47E-03	3.18E-03	2.38E-03	2.64E-03
Brain	4.31E-03	2.11E-03	2.97E-03	2.47E-03	2.15E-03	2.34E-03
Breasts	1.89E-03	1.31E-03	1.25E-03	1.80E-03	1.22E-03	1.35E-03
Gallbladder Wall	4.50E-03	5.36E-03	6.66E-03	6.21E-03	4.49E-03	7.68E-03
LLI Wall	2.91E-03	1.88E-03	1.93E-03	4.55E-03	2.14E-03	2.31E-03
Small Intestine	1.22E-02	8.05E-03	1.05E-02	3.62E-02	1.37E-02	1.32E-02
Stomach Wall	2.71E-03	1.89E-03	1.88E-03	3.08E-03	1.89E-03	2.09E-03
ULI Wall	5.92E-03	3.80E-03	4.65E-03	1.43E-02	5.61E-03	5.61E-03
Heart Wall	5.65E-03	1.06E-02	6.45E-03	9.05E-03	5.25E-03	5.13E-03
Kidneys	6.62E-03	4.73E-03	6.42E-03	7.25E-03	5.64E-03	9.22E-03
Liver	1.31E-02	9.95E-03	1.26E-02	1.12E-02	1.09E-02	1.14E-02
Lungs	4.26E-03	3.12E-03	3.49E-03	5.11E-03	3.90E-03	4.15E-03
Muscle	2.21E-03	1.47E-03	1.45E-03	2.33E-03	1.44E-03	1.60E-03
Ovaries	3.28E-03	2.07E-03	2.20E-03	5.39E-03	2.40E-03	2.58E-03
Pancreas	3.21E-03	2.39E-03	2.42E-03	3.31E-03	2.37E-03	2.62E-03
Red Marrow	5.63E-03	4.50E-03	4.13E-03	6.67E-03	4.59E-03	4.89E-03
Osteogenic Cells	5.40E-03	3.64E-03	3.40E-03	5.70E-03	3.60E-03	3.96E-03
Skin	1.73E-03	1.11E-03	1.09E-03	1.67E-03	1.06E-03	1.19E-03
Spleen	5.85E-03	7.16E-03	5.05E-03	3.97E-03	6.82E-03	7.23E-03

Formatted Table

1										
2										
3										
4										
5										
6										
7		03	03	03	03	03	03			
8	Testes	<u>1.92E-03</u>	<u>1.21E-03</u>	<u>1.15E-03</u>	<u>1.83E-03</u>	<u>1.13E-03</u>	<u>1.28E-03</u>			
9		03	03	03	03	03	03			
10	Thymus	<u>2.22E-03</u>	<u>1.63E-03</u>	<u>1.49E-03</u>	<u>2.15E-03</u>	<u>1.45E-03</u>	<u>1.60E-03</u>			
11		03	03	03	03	03	03			
12	Thyroid	<u>3.83E-03</u>	<u>2.65E-03</u>	<u>3.70E-03</u>	<u>5.14E-03</u>	<u>6.43E-03</u>	<u>3.90E-03</u>			
13	Urinary	03	03	03	03	03	03			
14	Bladder	<u>3.05E-03</u>	<u>1.85E-03</u>	<u>2.29E-03</u>	<u>3.67E-03</u>	<u>1.72E-03</u>	<u>2.08E-03</u>			
15	Wall	03	03	03	03	03	03			
16		<u>3.12E-03</u>	<u>1.95E-03</u>	<u>2.07E-03</u>	<u>4.84E-03</u>	<u>2.21E-03</u>	<u>2.39E-03</u>			
17	Uterus	03	03	03	03	03	03			
18	Total	<u>2.87E-03</u>	<u>1.99E-03</u>	<u>2.06E-03</u>	<u>3.20E-03</u>	<u>2.04E-03</u>	<u>2.23E-03</u>			
19	Body	03	03	03	03	03	03			
20										
21	ED	0.0039	0.0027	0.0030	0.0050	0.0034	0.0035			
22		3	9	5	9	6	4			
23								<u>mean</u>	<u>organ</u>	
24								<u>absorbe</u>	<u>doses</u>	
25								<u>d dose</u>	<u>from</u>	
26	<u>Subject</u>								<u>mean</u>	
27	<u>Nr.</u>	<u>1</u>	<u>2</u>	<u>3</u>	<u>4</u>	<u>5</u>	<u>6</u>		<u>TIAC</u>	
28										
29	Adrenals	<u>3.21E-03</u>	<u>2.38E-03</u>	<u>2.47E-03</u>	<u>3.18E-03</u>	<u>2.38E-03</u>	<u>2.64E-03</u>	<u>2.71E-03</u>	<u>2.78E-03</u>	<u>2.52%</u>
30		<u>4.31E-03</u>	<u>2.11E-03</u>	<u>2.97E-03</u>	<u>2.47E-03</u>	<u>2.15E-03</u>	<u>2.34E-03</u>	<u>2.73E-03</u>	<u>2.79E-03</u>	<u>2.33%</u>
31	Brain	<u>03</u>	<u>03</u>	<u>03</u>	<u>03</u>	<u>03</u>	<u>03</u>	<u>03</u>	<u>03</u>	
32		<u>1.89E-03</u>	<u>1.31E-03</u>	<u>1.25E-03</u>	<u>1.80E-03</u>	<u>1.22E-03</u>	<u>1.35E-03</u>	<u>1.47E-03</u>	<u>1.51E-03</u>	<u>2.65%</u>
33	Breasts	<u>03</u>	<u>03</u>	<u>03</u>	<u>03</u>	<u>03</u>	<u>03</u>	<u>03</u>	<u>03</u>	
34	Gallbladder	<u>4.50E-03</u>	<u>5.36E-03</u>	<u>6.66E-03</u>	<u>6.21E-03</u>	<u>4.49E-03</u>	<u>7.68E-03</u>	<u>5.82E-03</u>	<u>5.95E-03</u>	<u>2.24%</u>
35	er Wall	<u>03</u>	<u>03</u>	<u>03</u>	<u>03</u>	<u>03</u>	<u>03</u>	<u>03</u>	<u>03</u>	
36		<u>2.91E-03</u>	<u>1.88E-03</u>	<u>1.93E-03</u>	<u>4.55E-03</u>	<u>2.14E-03</u>	<u>2.31E-03</u>	<u>2.62E-03</u>	<u>2.64E-03</u>	<u>0.76%</u>
37	LLI Wall	<u>03</u>	<u>03</u>	<u>03</u>	<u>03</u>	<u>03</u>	<u>03</u>	<u>03</u>	<u>03</u>	
38	Small	<u>1.22E-02</u>	<u>8.05E-03</u>	<u>1.05E-02</u>	<u>3.62E-02</u>	<u>1.37E-02</u>	<u>1.32E-02</u>	<u>1.56E-02</u>	<u>1.57E-02</u>	<u>0.37%</u>
39	Intestine	<u>02</u>	<u>03</u>	<u>02</u>	<u>02</u>	<u>02</u>	<u>02</u>	<u>02</u>	<u>02</u>	
40	Stomach	<u>2.71E-03</u>	<u>1.89E-03</u>	<u>1.88E-03</u>	<u>3.08E-03</u>	<u>1.89E-03</u>	<u>2.09E-03</u>	<u>2.26E-03</u>	<u>2.30E-03</u>	<u>1.88%</u>
41	Wall	<u>03</u>	<u>03</u>	<u>03</u>	<u>03</u>	<u>03</u>	<u>03</u>	<u>03</u>	<u>03</u>	
42		<u>5.92E-03</u>	<u>3.80E-03</u>	<u>4.65E-03</u>	<u>1.43E-03</u>	<u>5.61E-03</u>	<u>5.61E-03</u>	<u>6.65E-03</u>	<u>6.64E-03</u>	<u>-0.13%</u>
43	ULI Wall	<u>03</u>	<u>03</u>	<u>03</u>	<u>02</u>	<u>03</u>	<u>03</u>	<u>03</u>	<u>03</u>	
44	Heart	<u>5.65E-03</u>	<u>1.06E-02</u>	<u>6.45E-03</u>	<u>9.05E-03</u>	<u>5.25E-03</u>	<u>5.13E-03</u>	<u>7.02E-03</u>	<u>7.40E-03</u>	<u>5.11%</u>
45	Wall	<u>03</u>	<u>02</u>	<u>03</u>	<u>03</u>	<u>03</u>	<u>03</u>	<u>03</u>	<u>03</u>	
46		<u>6.62E-03</u>	<u>4.73E-03</u>	<u>6.42E-03</u>	<u>7.25E-03</u>	<u>5.64E-03</u>	<u>9.22E-03</u>	<u>6.65E-03</u>	<u>6.96E-03</u>	<u>4.50%</u>
47	Kidneys	<u>03</u>	<u>03</u>	<u>03</u>	<u>03</u>	<u>03</u>	<u>03</u>	<u>03</u>	<u>03</u>	
48		<u>1.31E-03</u>	<u>9.95E-03</u>	<u>1.26E-03</u>	<u>1.12E-03</u>	<u>1.09E-03</u>	<u>1.14E-03</u>	<u>1.15E-03</u>	<u>1.21E-03</u>	<u>4.75%</u>
49	Liver	<u>02</u>	<u>03</u>	<u>02</u>	<u>02</u>	<u>02</u>	<u>02</u>	<u>02</u>	<u>02</u>	
50		<u>4.26E-03</u>	<u>3.12E-03</u>	<u>3.49E-03</u>	<u>5.11E-03</u>	<u>3.90E-03</u>	<u>4.15E-03</u>	<u>4.01E-03</u>	<u>4.14E-03</u>	<u>3.26%</u>
51	Lungs	<u>03</u>	<u>03</u>	<u>03</u>	<u>03</u>	<u>03</u>	<u>03</u>	<u>03</u>	<u>03</u>	
52		<u>2.21E-03</u>	<u>1.47E-03</u>	<u>1.45E-03</u>	<u>2.33E-03</u>	<u>1.44E-03</u>	<u>1.60E-03</u>	<u>1.75E-03</u>	<u>1.78E-03</u>	<u>1.69%</u>
53	Muscle	<u>03</u>	<u>03</u>	<u>03</u>	<u>03</u>	<u>03</u>	<u>03</u>	<u>03</u>	<u>03</u>	
54		<u>3.28E-03</u>	<u>2.07E-03</u>	<u>2.20E-03</u>	<u>5.39E-03</u>	<u>2.40E-03</u>	<u>2.58E-03</u>	<u>2.99E-03</u>	<u>3.00E-03</u>	<u>0.44%</u>
55	Ovaries	<u>03</u>	<u>03</u>	<u>03</u>	<u>03</u>	<u>03</u>	<u>03</u>	<u>03</u>	<u>03</u>	

	<u>3.21E-</u>	<u>2.39E-</u>	<u>2.42E-</u>	<u>3.31E-</u>	<u>2.37E-</u>	<u>2.62E-</u>	<u>2.72E-</u>	<u>2.78E-</u>	<u>2.16%</u>
<u>Pancreas</u>	<u>03</u>	<u>03</u>	<u>03</u>	<u>03</u>	<u>03</u>	<u>03</u>	<u>03</u>	<u>03</u>	
<u>Red</u>	<u>5.63E-</u>	<u>4.50E-</u>	<u>4.13E-</u>	<u>6.67E-</u>	<u>4.59E-</u>	<u>4.89E-</u>	<u>5.07E-</u>	<u>5.24E-</u>	<u>3.28%</u>
<u>Marrow</u>	<u>03</u>	<u>03</u>	<u>03</u>	<u>03</u>	<u>03</u>	<u>03</u>	<u>03</u>	<u>03</u>	
<u>Osteogeni</u>	<u>5.40E-</u>	<u>3.64E-</u>	<u>3.40E-</u>	<u>5.70E-</u>	<u>3.60E-</u>	<u>3.96E-</u>	<u>4.28E-</u>	<u>4.40E-</u>	<u>2.65%</u>
<u>c Cells</u>	<u>03</u>	<u>03</u>	<u>03</u>	<u>03</u>	<u>03</u>	<u>03</u>	<u>03</u>	<u>03</u>	
	<u>1.73E-</u>	<u>1.11E-</u>	<u>1.09E-</u>	<u>1.67E-</u>	<u>1.06E-</u>	<u>1.19E-</u>	<u>1.31E-</u>	<u>1.33E-</u>	<u>1.63%</u>
<u>Skin</u>	<u>03</u>	<u>03</u>	<u>03</u>	<u>03</u>	<u>03</u>	<u>03</u>	<u>03</u>	<u>03</u>	
	<u>5.85E-</u>	<u>7.16E-</u>	<u>5.05E-</u>	<u>3.97E-</u>	<u>6.82E-</u>	<u>7.23E-</u>	<u>6.01E-</u>	<u>6.45E-</u>	<u>6.77%</u>
<u>Spleen</u>	<u>03</u>	<u>03</u>	<u>03</u>	<u>03</u>	<u>03</u>	<u>03</u>	<u>03</u>	<u>03</u>	
	<u>1.92E-</u>	<u>1.21E-</u>	<u>1.15E-</u>	<u>1.83E-</u>	<u>1.13E-</u>	<u>1.28E-</u>	<u>1.42E-</u>	<u>1.45E-</u>	<u>2.07%</u>
<u>Testes</u>	<u>03</u>	<u>03</u>	<u>03</u>	<u>03</u>	<u>03</u>	<u>03</u>	<u>03</u>	<u>03</u>	
	<u>2.22E-</u>	<u>1.63E-</u>	<u>1.49E-</u>	<u>2.15E-</u>	<u>1.45E-</u>	<u>1.60E-</u>	<u>1.76E-</u>	<u>1.80E-</u>	<u>2.41%</u>
<u>Thymus</u>	<u>03</u>	<u>03</u>	<u>03</u>	<u>03</u>	<u>03</u>	<u>03</u>	<u>03</u>	<u>03</u>	
	<u>3.83E-</u>	<u>2.65E-</u>	<u>3.70E-</u>	<u>5.14E-</u>	<u>6.43E-</u>	<u>3.90E-</u>	<u>4.28E-</u>	<u>4.31E-</u>	<u>0.81%</u>
<u>Thyroid</u>	<u>03</u>	<u>03</u>	<u>03</u>	<u>03</u>	<u>03</u>	<u>03</u>	<u>03</u>	<u>03</u>	
<u>Urinary</u>							<u>2.44E-</u>	<u>2.44E-</u>	<u>-0.14%</u>
<u>Bladder</u>	<u>3.05E-</u>	<u>1.85E-</u>	<u>2.29E-</u>	<u>3.67E-</u>	<u>1.72E-</u>	<u>2.08E-</u>	<u>03</u>	<u>03</u>	
<u>Wall</u>	<u>03</u>	<u>03</u>	<u>03</u>	<u>03</u>	<u>03</u>	<u>03</u>			
	<u>3.12E-</u>	<u>1.95E-</u>	<u>2.07E-</u>	<u>4.84E-</u>	<u>2.21E-</u>	<u>2.39E-</u>	<u>2.76E-</u>	<u>2.78E-</u>	<u>0.60%</u>
<u>Uterus</u>	<u>03</u>	<u>03</u>	<u>03</u>	<u>03</u>	<u>03</u>	<u>03</u>	<u>03</u>	<u>03</u>	
<u>Total</u>	<u>2.87E-</u>	<u>1.99E-</u>	<u>2.06E-</u>	<u>3.20E-</u>	<u>2.04E-</u>	<u>2.23E-</u>	<u>2.40E-</u>	<u>2.46E-</u>	<u>2.51%</u>
<u>Body</u>	<u>03</u>	<u>03</u>	<u>03</u>	<u>03</u>	<u>03</u>	<u>03</u>	<u>03</u>	<u>03</u>	
	<u>0.0039</u>	<u>0.0027</u>	<u>0.0030</u>	<u>0.0050</u>	<u>0.0034</u>	<u>0.0035</u>	<u>0.00364</u>	<u>0.0038</u>	<u>5.86%</u>
<u>ED</u>	<u>3</u>	<u>9</u>	<u>5</u>	<u>9</u>	<u>6</u>	<u>4</u>	<u>3</u>	<u>7</u>	